International Journal of Recent Development in Engineering and Technology
Website: www.ijrdet.com (ISSN 2347-6435 (Online) Volume 15, Issue 08, August 2026)

Deep Learning Model for Pnuemonia Diagnosis using CNN

Umejuru Daniel[1], Promise Jumbo[2], Ohia Paul Ndudiri[3]

[1]*Department of Computer Science, University of Port Harcourt, Choba, Nigeria*
[2,3]*Department of Information Technology, University of Port Harcourt, Choba, Nigeria*

Abstract-- **This research work proposes a Convolutional Neural Network (CNN) model built in order, and to recognize the presence of pneumonia in a dataset of chest X-beam pictures. Unlike different strategies that depend entirely on transfer learning which draws near or customary high quality methods to accomplish remarkable order execution, this review developed a CNN model from the beginning but utilizing transfer learning and information increase to separate provisions from a given chest X-beam picture and group it to decide whether an individual is has pneumonia. The assessment result shows that the model made aggregate of (3,000) expectations (e.g., 3,000 patients were being tested for the presence of pneumonia). Out of the 3,000 cases, the proposed model detected 1628 patients as pneumonia positive, and 1372 patients as pneumonia negative. In all actuality, 1618 patients in the example dataset have the infection, and 1382 patients don't. The proposed model has a summary of precision 0.986%, an AUC ROC of 0.996%, an accuracy of 0.984%, and also a recall of 0.990% which beats cutting edge strategies. Moreover, these discoveries support the adequacy of the proposed procedure. This outcome shows that the proposed model can possibly and productively determine pneumonia to have extremely minor bogus positive rate. The executed model was done using Python programming language including some applications utilizing web innovations like cup system, Cascading Style Sheet (CSS), JavaScript, and Hypertext Mark-up Language (HTML).**

Keywords-- **Deep Learning, Mechanical Process Automation, MRI, Processed Tomography, CNN, Diagnosis,**

I. Introduction

Many individuals are in danger of contracting pneumonia, and the danger is particularly high in emerging nations where individuals depend on contaminating types of energy [2]. The World Health Organization (WHO) appraises that family air contamination related illnesses, for example, pneumonia cause more than 4,000,000 unexpected losses every year. Pneumonia is quite possibly the most genuine disease that kills most of grown-ups around the world. As indicated by Health Metrics and Evaluation (IHME), individuals matured 70 and more established had the most elevated pneumonia death rates in 2020. Consistently, more than 1.13 million pneumonia-related passings are accounted for in this age bunch [3].

Pneumonia is an incendiary reaction that happens in the lung sacs known as alveoli. It is often brought about by organisms, infections, microorganisms, and different organisms. As the microbes approach the lung, white platelets assault them, causing irritation in the sacs. Accordingly, pneumonia liquid fills the alveoli, causing indications, for example, trouble breathing, fever, and hacking. On the off chance that the contamination isn't recognized and treated from the get-go in the sickness' movement, it can spread all through the body, bringing about the patient's passing because of a powerlessness to trade gas in the lungs. Pneumonia is a genuine illness that can possibly cause serious harm in a brief timeframe because of the progression of liquid in the lungs, which brings about suffocating [1]. The significance of early analysis in the treatment interaction couldn't possibly be more significant.

The most widely recognized strategy for diagnosing pneumonia is with a CT output, radiography, or a MRI. Conclusions can be emotional for an assortment of reasons, including the presence of illness, which can be darkened in chest X-beam pictures or mistook for different sicknesses. Clinical experts analyze the patient's chest X-beam or radiograph to decide if they are tainted with the infection [5]. Besides, research center outcomes or the patient's clinical history are regularly used to analyze pneumonia. X-beams are utilized to enter chest radiography, where hard tissues, for example, bones produce brilliant shading and delicate tissues produce a dull shading [7] Patients with pneumonia have liquids swirling around sacs of their lungs in their chest cavity, and their x-beam pictures seem more splendid. An assortment of anomalies might be seen in the lung cavities, with more splendid shadings addressing vein enlarging, disease cells, and heart irregularities [9].

II. Pneumonia And Artificial Intelligence

Pneumonia is an infectious sickness that causes lung ulcers and is one of the main sources of death in youngsters and the old all throughout the planet [4]. Pneumonia represents around 18% of all passings in kids younger than five around the world.

International Journal of Recent Development in Engineering and Technology
Website: www.ijrdet.com (ISSN 2347-6435 (Online) Volume 15, Issue 08, August 2026)

Moreover, around two individuals overall are influenced by this illness every year, and passing can happen if proactive move isn't made. It is basic to analyze pneumonia quickly [8].To stay away from misdiagnosis, a specialist radiologist should play out a proactive and proficient analysis utilizing chest X-beams. Chest X-beams are the most reasonable and generally utilized strategy for diagnosing and treating pneumonia [6]. Important bodily functions, lab tests, and clinical history are utilized to affirm the conclusion. The presence of different conditions in the lungs, like volume misfortune, liquid over-burden, cellular breakdown in the lungs and dying, careful or post-radiation changes, entangles the conclusion of pneumonia by means of chest X-beam. In view of the idea of chest X-beam picture examination, pneumonia analyze through X-beam pictures are habitually uncertain and can be mistaken for different infections with comparable components, like depression, haziness, radiations, and pleural. Accordingly, chest X-beams can't be utilized as effectively to recognize pneumonia [10]. At the point when accessible, an examination of the patient's chest X-beams got at various time focuses, just as connection with clinical side effects and history, can support conclusion. An assortment of components, like patient situating and profundity of motivation, can adjust the presence of the CXR, further entangling understanding. [12].

Artificial intelligence is an expansive logical discipline with establishes in way of thinking, arithmetic, and software engineering that tries to comprehend and foster frameworks with knowledge like properties [11]. Man-made intelligence is the reenactment of human insight in machines that are intended to imitate intellectual capacities that people partner with other human personalities, for example, learning and critical thinking. Simulated intelligence can possibly change the wellbeing area by expanding adequacy and effectiveness, making headroom for all inclusive wellbeing inclusion, and further developing results [13]. The fast progression of AI and related innovations will empower medical care suppliers to offer new benefit to their patients while additionally working on the productivity of their functional cycles [15]. In case AI is generally used to help medical care administrations, it can possibly guarantee both quality medical care and massive expense reserve funds.

The progression of innovation in the field of computerized reasoning (AI) permits us to work on the speed and proficiency with which we analyze different kinds of issues. The ascent of convolutional neural organizations lately has been especially recognizable, with promising outcomes in picture handling and PC vision issues [16]. Considering that people have a restricted capacity to recognize designs in individual pictures, even clinical experts might battle to make an exact analysis. To diminish the quantity of mistakes and potentially negative side-effects, PC programs dependent on AI standards are progressively being utilized as indicative collaborator devices in medication [17].

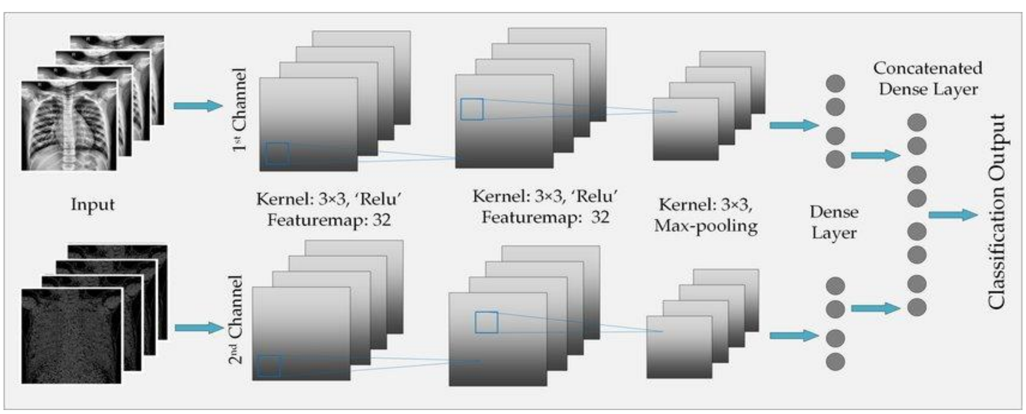

Figure 1: CNN Architecture (Source: Kelly 2020)

2.1 Deep exchange learning

CNNs normally beat in bigger datasets than in more modest ones. Move learning can be helpful in CNN applications where the dataset isn't huge.

Figure 2 portrays the idea of move learning, wherein a prepared model from a huge dataset, like ImageNet, is applied to a more modest dataset [18].

Move learning has as of late been utilized effectively in an assortment of field applications like assembling, medication, and things screening [18].

This wipes out the requirement for a huge dataset and abbreviates the preparation time frame needed by the profound taking in calculation when created without any preparation.

Figure 2: Transfer Learning Architecture (Source: Wang et al 2020)

III. METHODOLOGY

This section examines the strategy of this examination work. It additionally examines the proposed model, information gathering, necessity determination, examination and plan of the proposed model.

Likewise, reflected in the proposed structure is the utilization of profound learning procedure for performing effective pneumonia recognition. The work process of the procedure is shown Figure 3

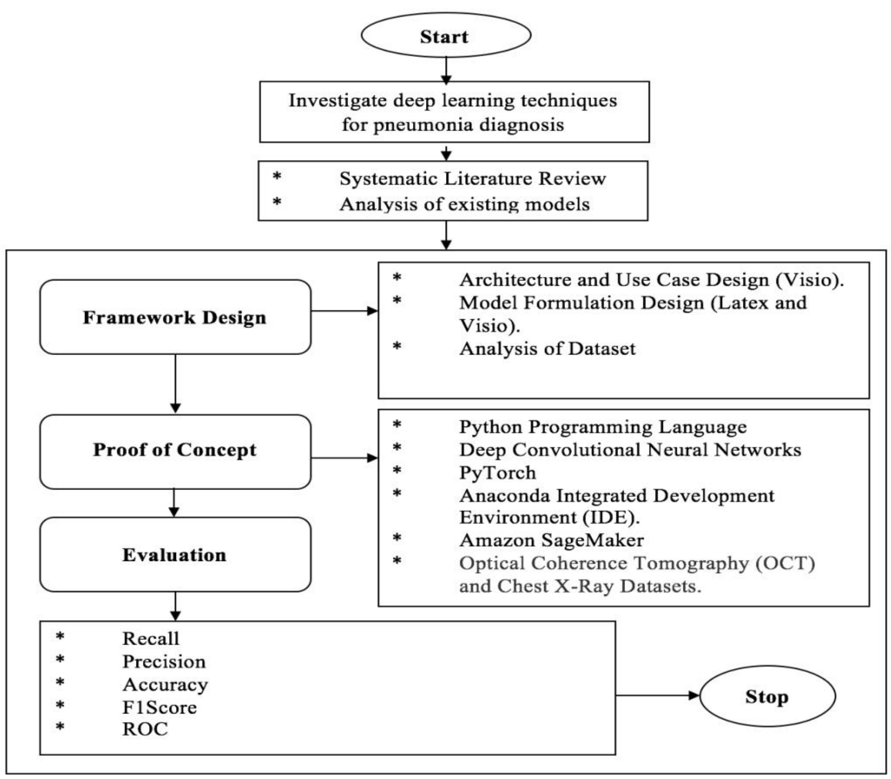

Figure 3: Methodology Workflow

International Journal of Recent Development in Engineering and Technology
Website: www.ijrdet.com (ISSN 2347-6435 (Online) Volume 15, Issue 08, August 2026)

Figure 3 explains the system work and process of this exploration work, the outlined strategy. This exploration work will examine profound learning methods in distinguishing pneumonia utilizing chest X-beam picture dataset. The proposed reasonable system would be planned utilizing Deep Convolutional Neural Networks, and element will be done to decrease the underlying crude arrangement of information to a sensible gathering for handling, since highlights that are inappropriately chosen will have adverse consequence on our model

3.1 The Proposed Model

A productive answer for the identification of pneumonia from chest X-beams picture dataset is proposed in this review. The argumentation of information was utilized to resolve the issue of the restricted dataset, and afterward, Deep Convolutional Neural Networks, as examined in Section 3.2, was calibrated for pneumonia characterization. Then, at that point, forecasts from these models were consolidated, utilizing a weighted classifier to figure the last expectation. The theoretical casing of the proposed model can be found in Figure 4.

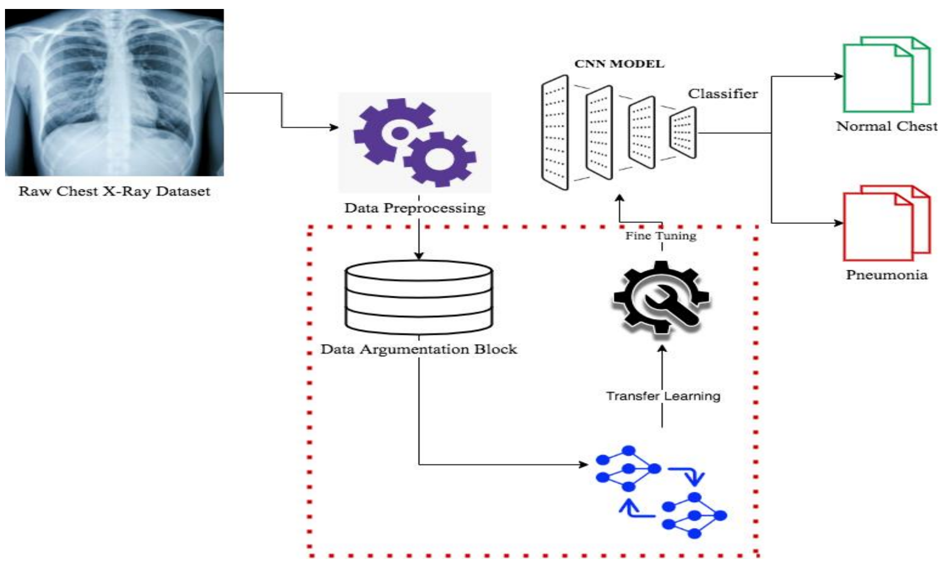

Figure 4: Proposed Model

3.2 Dataset Gathering and Description

The dataset was acquired from kaggle. The dataset is partitioned into three envelopes (preparing set, testing set, and approval set) and contains subfolders for each picture classification (Pneumonia/Normal). There are 5,863 X-Ray pictures (JPEG) and two classes (Pneumonia/Normal). Chest X-beam pictures (front back) were browsed review companions of pediatric patients matured one to five years of age at Guangzhou Women and Children's Medical Center in Guangzhou. To start the investigation of chest x-beam pictures, all chest radiographs were at first evaluated for quality control by eliminating any sweeps that were of low quality or were disjointed.

Prior to preparing the AI framework, the analyses for the pictures were reviewed by two master doctors. A third master additionally inspected the assessment set to represent any reviewing blunders. The ordinary chest X-beam (left board) shows clear lungs without any spaces of strange opacification. Bacterial pneumonia (center) is described by a central lobar solidification, for this situation in the right upper projection (white bolts), though popular pneumonia (right) is portrayed by a more diffuse "interstitial" design in the two lungs, as displayed in Figure 5.

International Journal of Recent Development in Engineering and Technology
Website: www.ijrdet.com (ISSN 2347-6435 (Online) Volume 15, Issue 08, August 2026)

Figure 5: Sample Dataset with normal, bacterial pneumonia and viral pneumonia

3.3 Data Pre-handling and Argumentation

To make the dataset reasonable for our model, each picture must be pre-handled. There were two basic advances: resizing and standardization. Every one of the pictures were standardized utilizing our profound learning design. The information seems, by all accounts, to be unequal. We will utilize information expansion to build the quantity of preparing models. To stay away from the overfitting issue, we falsely extended our dataset by making the current dataset considerably bigger. To recreate the varieties, the preparation information is modified with little changes. Information expansion strategies are approaches that change the preparation information in manners that change the cluster portrayal while keeping the name something very similar. Grayscales, even and vertical flips, arbitrary harvests, shading nerves, interpretations, revolutions, and numerous different expansions are famous. The analysts can without much of a stretch twofold or triple the quantity of preparing models and make an exceptionally powerful model by applying only several these changes to our preparation information. The dataset is portrayed in Table 1.

Table 1: Number of Pneumonia and Normal Images in the preparation and testing sets of the first dataset

Class Name	Training Set	Testing Set
Normal	1341 624	1965
Pneumonia	3875 624	4499
Total	5216 12486464	

3.4 Data Augmentation and Preprocessing

A few information expansion techniques were utilized to misleadingly expand the size of the dataset, and the dataset quality was preprocessed to support the goal of overfitting issues and to further develop the model speculation capacity during preparing. Table 2 shows the picture augmentation settings that were utilized. During the increase cycle, the rescale activity addresses picture decrease or amplification. The turn range, which is 40 degrees, indicates the reach wherein the pictures were haphazardly pivoted during preparing. Width shift is a 20% even interpretation of the pictures, and stature shift is a 20% vertical interpretation of the pictures. Besides, a shear scope of 20% cut the picture points a counter clockwise way. The zoom ran-ge arbitrarily zooms the pictures to a proportion of 20%, and the pictures are then flipped evenly. The preprocessed pneumonia picture dataset is displayed in Figure 6.

International Journal of Recent Development in Engineering and Technology
Website: www.ijrdet.com (ISSN 2347-6435 (Online) Volume 15, Issue 08, August 2026)

Table 2: Image Dataset Augmentation Setup

Approach	Settings
Range of Rotation	40
Rescale	1/128
Zoom Range	20 percent
Shear Range	20 percent
Height Shift	20 percent
Width Shift	20 percent
Horizontal Flip	True

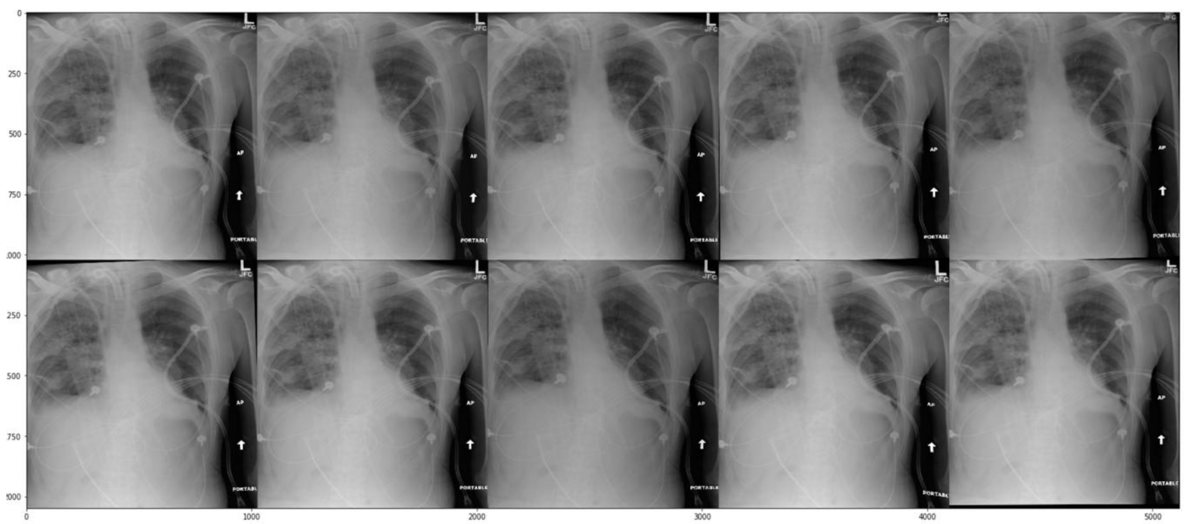

Figure 6: Sample Pre-processed Image Dataset

3.5 Problem Definition of the Weighted Classifier

In the proposed model, a weight (W_k) compare to each demonstrate. W_k can be characterized as the faith in the model, with k addressing the pre-prepared model. (W_k) has the qualities somewhere in the range of 0 and 1, and the amount of all weight is 1 as displayed in (Equation (2)). After the model was fine- tuned, it retuned the likelihood for each class name, for example, two classes as a grid (P_k). A weighted amount of the expectation is displayed in (Equation (1)).

$$P_1 W_1+P_2 W_2+P_3 W_3+\cdots+P_k W_k= P_f \quad (1)$$

$$W_1+W_2+W_3+\cdots+W_k=1 \quad (2)$$

$$Loss=-1/N \sum_{i=1}^{n} [y\times\log(p)+(1-y)\times\log(1-p)] \quad (3)$$

P_k addresses the expectation grid, with the shape portraying the quantity of streamlining pictures comparing to the design.

In (Equation (1)), the commitment of the model is weighted by a coefficient (W_k), which demonstrates the confidence in the model. (P_k) was gotten for the inconspicuous picture set in the model. Then, at that point (Equation (1)) was advanced with the end goal that the characterization mistake will be limited and (Equation (2)) was likewise fulfilled. Differential advancement was used for worldwide enhancement in (Equation (1)). Differential advancement is a stochastic worldwide pursuit calculation. It was utilized to advanced (Equation (1)) by iteratively refining an up-and-comer arrangement with respect to Equation (2)). Thus, improving (Equation (1)) would give the W_k esteems comparing to our model. The worth of W_k for the k^{th} model relied upon our model presentation on the dataset. The greatest cycles for our differential development strategy were kept to be 1000. With the assistance of P_f, the forecast of a class name could be registered. Characterization misfortune relating to the P_f was diminished while advancing (Equation (1)).

Log misfortune (Equation (3)), likewise known a cross-entropy misfortune or strategic misfortune was used as the misfortune work. In (Equation (3)), N signifies the size of the picture set and p dnotes the likelihood that the given picture is pneumonia positive. Figure 7 delineates the cycle used to track down the ideal weight relating to our model.

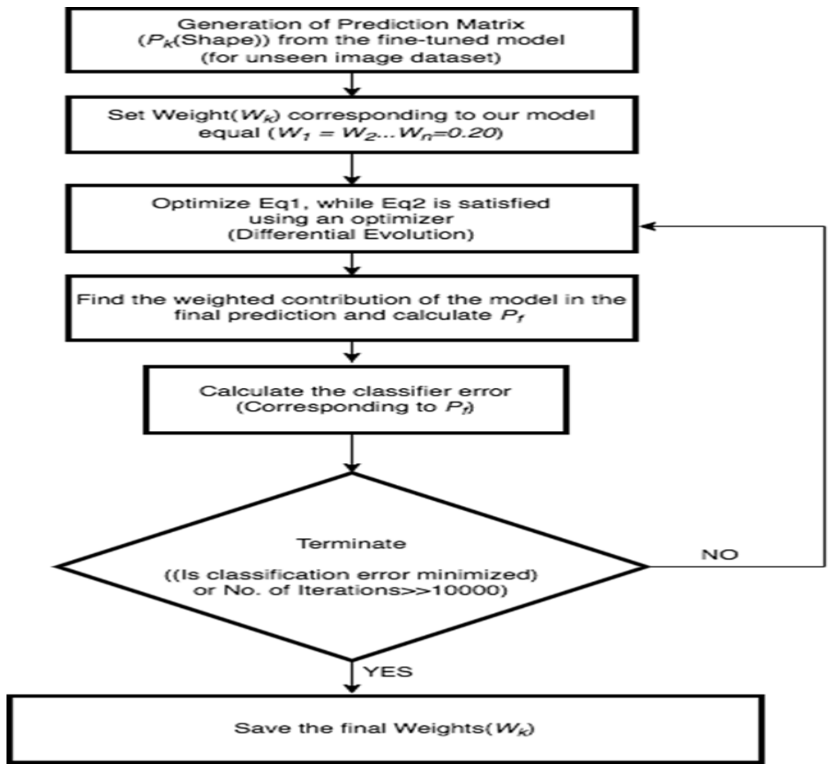

Figure 7: Process of Calculating Weight

3.6 Design of the Class Activation Map Framework

The class initiation guide can help in demystifying the aftereffects of our profound learning model. Customarily, profound learning-based techniques are viewed as a discovery approach. For clinical dynamic like pneumonia finding, it is vital that the aftereffects of our model can be deciphered. The class enactment guide can help in recognizing the pieces of our dataset on which the model was centering while at the same time making the last forecast and thus can give experiences into the working of the model.

Such an investigation can additionally help in hyper boundary tuning and gain comprehension of the explanation for the disappointment of the model. For acquiring the class actuation map, the organization should have been prepared with the worldwide normal pooling layer. After the worldwide normal pooling layer, a completely associated network was kept up with, which was trailed by the SoftMax layer, giving the class, like pneumonia, as shown in Figure8.

International Journal of Recent Development in Engineering and Technology
Website: www.ijrdet.com (ISSN 2347-6435 (Online) Volume 15, Issue 08, August 2026)

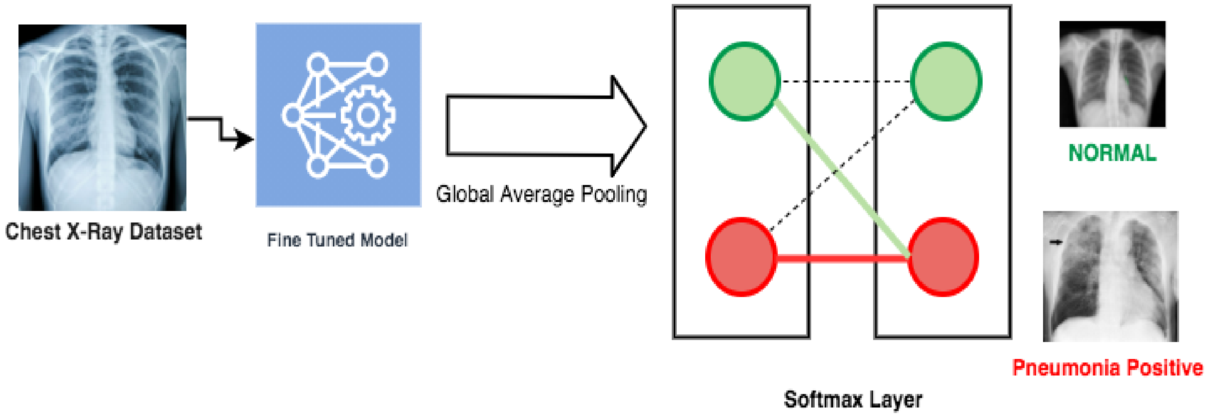

Figure 8: Class Activation Map Framework

3.7 Analysis of Performance Metrics

After the preparation stage, the carried out model will be scrutinized on the test dataset. The exactness, review, accuracy, F1, and region under the bend (AUC) scores would be used to approve the presentation. While arranging sound and pneumonia patients, genuine positive (TP) means the quantity of pneumonia pictures inaccurately recognized as pneumonia, genuine negative (TN) signifies the quantity of typical pictures erroneously distinguished as expected (solid), and bogus positive (FP) indicates the quantity of ordinary pictures mistakenly distinguished as pneumonia pictures, and the quantity of pneumonia pictures wrongly named as ordinary is alluded to as bogus negative (FN) in the definitions and conditions underneath.

Exactness: precision portrays how intently a deliberate worth matches a known worth.

Accuracy= (TP+FN)/ ((TP+TF+FP+FN))

AUC Score and ROC Curve: AUC (region under bend) shows the level of distinctness, though ROC (beneficiary working attributes) is a likelihood bend. The ROC bend is a chart that shows the connection between affectability (genuine positive rate) and particularity (pace of bogus up-sides) (bogus positive rate).

Review: It works out the measure of genuine up-sides the model had the option to catch in the wake of being named accordingly (genuine positive).

Recall=TP/((TP+FN))

Accuracy: This measurement demonstrates how precise the model is in anticipating positive results.

TP/((TP+FP))

F1 Score: It accomplishes a decent mix of accuracy and review.

F1=2× ((Precision×Recall))/((Precision+Recall))

International Journal of Recent Development in Engineering and Technology
Website: www.ijrdet.com (ISSN 2347-6435 (Online) Volume 15, Issue 08, August 2026)

IV. RESULTS

```
!nvidia-smi

Sat Aug  7 20:48:26 2021
+-----------------------------------------------------------------------------+
| NVIDIA-SMI 470.42.01    Driver Version: 460.32.03    CUDA Version: 11.2     |
|-------------------------------+----------------------+----------------------+
| GPU  Name        Persistence-M| Bus-Id        Disp.A | Volatile Uncorr. ECC |
| Fan  Temp  Perf  Pwr:Usage/Cap|         Memory-Usage | GPU-Util  Compute M. |
|                               |                      |               MIG M. |
|===============================+======================+======================|
|   0  Tesla T4            Off  | 00000000:00:04.0 Off |                    0 |
| N/A   51C    P8    10W /  70W |      0MiB / 15109MiB |      0%      Default |
|                               |                      |                  N/A |
+-------------------------------+----------------------+----------------------+

+-----------------------------------------------------------------------------+
| Processes:                                                                  |
|  GPU   GI   CI        PID   Type   Process name                  GPU Memory |
|        ID   ID                                                   Usage      |
|=============================================================================|
|  No running processes found                                                 |
+-----------------------------------------------------------------------------+
```

Figure 9: Google Colab on Cloud for Training Deep Learning Models

```python
def proof_of_concept_cnn_model():
    model = tf.keras.Sequential([
        tf.keras.layers.Conv2D(32, kernel_size=(3,3), strides=(1,1), padding = 'valid', activation = 'relu', input_
        tf.keras.layers.MaxPool2D(pool_size=(2,2)), # Flatten Output of Convolutional Layer

        tf.keras.layers.Conv2D(32, kernel_size=(3,3), strides=(1,1), padding = 'valid', activation = 'relu'), #  co
        tf.keras.layers.MaxPool2D(pool_size=(2,2)), # Flatten Output of Convolutional Layer
        tf.keras.layers.Dropout(0.3),

        tf.keras.layers.Conv2D(64, 3, activation = 'relu', padding = 'valid'),
        tf.keras.layers.Conv2D(128, 3, activation = 'relu', padding = 'valid'),
        tf.keras.layers.BatchNormalization(),
        tf.keras.layers.MaxPool2D(),
        tf.keras.layers.Dropout(0.4),

        tf.keras.layers.Flatten(), # Flatten Output of  Convolutional Layer
        tf.keras.layers.Dense(512, activation = "relu"), # Hidden Layer
        tf.keras.layers.BatchNormalization(),
        tf.keras.layers.Dropout(0.5),
        tf.keras.layers.Dense(128, activation = "relu"), #  Output Layer
        tf.keras.layers.BatchNormalization(),
        tf.keras.layers.Dropout(0.5),
        tf.keras.layers.Dense(1, activation = "sigmoid")])

    return model
```

Figure 10: Model Implementation Code Snippet

Table 3: Output of the proposed CNN model architecture

Layer (type)	Output Shape	Param #
conv2d (Conv2D)	(None, 126, 126, 32)	896
max_pooling2d (MaxPooling2D)	(None, 63, 63, 32)	0
conv2d_1 (Conv2D)	(None, 61, 61, 32)	9248
max_pooling2d_1 (MaxPooling2	(None, 30, 30, 32)	0
dropout (Dropout)	(None, 30, 30, 32)	0

International Journal of Recent Development in Engineering and Technology
Website: www.ijrdet.com (ISSN 2347-6435 (Online) Volume 15, Issue 08, August 2026)

conv2d_2 (Conv2D)	(None, 28, 28, 64)	18496
conv2d_3 (Conv2D)	(None, 26, 26, 128)	73856
batch_normalization (BatchNo	(None, 26, 26, 128)	512
max_pooling2d_2 (MaxPooling2	(None, 13, 13, 128)	0
dropout_1 (Dropout)	(None, 13, 13, 128)	0
flatten_1 (Flatten)	(None, 21632)	0
dense_2 (Dense)	(None, 512)	11076096
batch_normalization_1 (Batch	(None, 512)	2048
dropout_2 (Dropout)	(None, 512)	0
dense_3 (Dense)	(None, 128)	65664
batch_normalization_2 (Batch	(None, 128)	512
dropout_3 (Dropout)	(None, 128)	0
dense_4 (Dense)	(None, 1)	129

Total params: 11,247,457
Trainable params: 11,245,921
Non-trainable params: 1,536

4.1 Model Training

Figure 11 shows that the preparation dataset was parted into preparing and approval set. 20% was utilized for the approval set, while 80% was utilized for the preparation set.

The model was additionally set to execute for thirty (30) age with (64) clump size. The absolute boundary is 11,247,457, the teachable boundary is 11,245,921, while the non-teachable boundary is 1,536 as shown in Table 2. The preparation model yield is displayed in Table 4.

International Journal of Recent Development in Engineering and Technology
Website: www.ijrdet.com (ISSN 2347-6435 (Online) Volume 15, Issue 08, August 2026)

```
#Model Training
history_mn = model_mn.fit(train_X_rgb,
                          train_Y,
                          epochs = 30,
                          validation_split = 0.20,
                          class_weight = classWeight,
                          batch_size = 64,
                          callbacks = [checkpoint_cb, early_stopping_cb, lr_scheduler])
```

Figure 11: Code Snippet of the training dataset

Table 4: Training Model Output

Epoch 1/30

63/63 [==============================] - 50s 733ms/step - loss: 0.1880 - accuracy: 0.9002 - precision: 0.8759 - recall : 0.9653 - AUC: 0.9560 - val_loss: 0.0549 - val_accuracy: 0.9840 - val_precision: 0.9903 - val_recall: 0.9789 - val_AUC: 0.996 6

Epoch 2/30

63/63 [==============================] - 44s 695ms/step - loss: 0.0420 - accuracy: 0.9860 - precision: 0.9814 - recall : 0.9931 - AUC: 0.9980 - val_loss: 0.0458 - val_accuracy: 0.9880 - val_precision: 0.9848 - val_recall: 0.9923 - val_AUC: 0.997 6

Epoch 3/30

63/63 [==============================] - 43s 685ms/step - loss: 0.0334 - accuracy: 0.9898 - precision: 0.9848 - recall : 0.9962 - AUC: 0.9977 - val_loss: 0.0425 - val_accuracy: 0.9900 - val_precision: 0.9923 - val_recall: 0.9885 - val_AUC: 0.997 1

Epoch 4/30

63/63 [==============================] - 43s 691ms/step - loss: 0.0263 - accuracy: 0.9938 - precision: 0.9905 - recall : 0.9982 - AUC: 0.9985 - val_loss: 0.0431 - val_accuracy: 0.9880 - val_precision: 0.9942 - val_recall: 0.9827 - val_AUC: 0.997 4

Epoch 5/30

63/63 [==============================] - 43s 684ms/step - loss: 0.0223 - accuracy: 0.9945 - precision: 0.9913 - recall : 0.9985 - AUC: 0.9990 - val_loss: 0.0390 - val_accuracy: 0.9890 - val_precision: 0.9923 - val_recall: 0.9866 - val_AUC: 0.997 3

Table 5: Confusion Matrix Table

N = ?	Predicted: NO	Predicted: YES
Actual: NO	TN = ?	FP = ?
Actual: YES	FN = ?	TP= ?

```
from sklearn.metrics import confusion_matrix

y_pred = model_mn.predict_classes(test_X_rgb)
confusion_matrix(test_Y, y_pred)
```

```
array([[1356,   26],
       [  16, 1602]])
```

Figure 12: Confusion Matrix of the Proposed Model

Figure 12 outline the disarray network for the proposed model dependent on information increase and move learning (CNN). The assessment result shows that the model made a sum of (3,000) expectations (e.g., 3,000 patients were being tried for the presence of pneumonia).

Out of the 3,000 cases, the proposed model anticipated 1628 patients as pneumonia positive, and 1372 patients as pneumonia negative. In all actuality, 1618 patients in the example dataset have the sickness, and 1382 patients don't. This outcome shows that the proposed model can possibly effectively determine pneumonia to have exceptionally minor bogus positive rate.

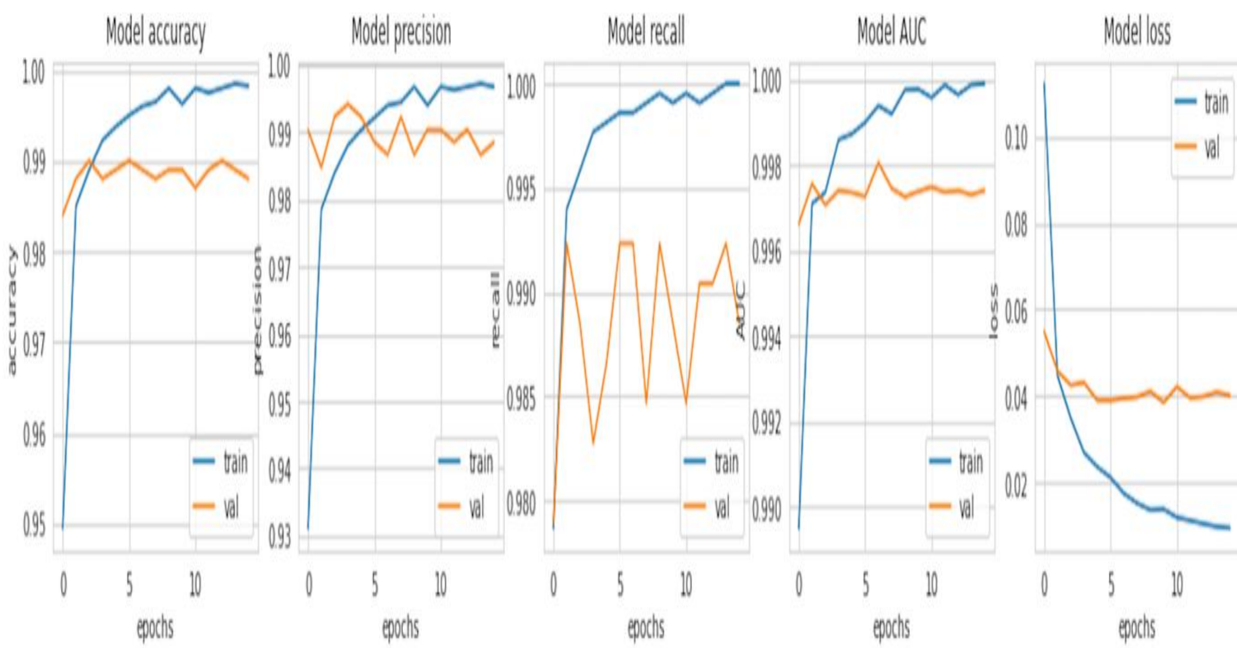

Figure 13: Performance of the Proposed Model

International Journal of Recent Development in Engineering and Technology
Website: www.ijrdet.com (ISSN 2347-6435 (Online) Volume 15, Issue 08, August 2026)

Figure 13 and Table 6 show the preparation exactness, model accuracy, model review, model AUC and model misfortune bends for the carried out model. The outcome of figure 13 shows the advancement of the outcomes in the bends. This implies that the class circulation in the preparation and approval is more fitting for preparing the proposed model. Moreover, it approves the viability of more learning and information expansion strategies in further developing the preparation interaction and model proficiency.

The consequences of the assessment measurements are processed utilizing the disarray networks in Figure 11. Tables 5 show the trial consequences of the verification of-idea assessment measurements. As indicated by Tables 5, the proposed model has an exhibition exactness of 0.986, an AUC of 0.996, an accuracy of 0.984, and a review of 0.990. Besides, these discoveries support the viability of the proposed strategy.

Table 6: Performance Metric Table

Accuracy	AUC	Precision	Recall
0.986	0.996	0.984	0.990

4.2 Benchmarking with State-of-the-craftsmanship Techniques

The proposed approach was benchmarked with cutting edge approaches and models. The proposed model proficiency was researched utilizing execution exactness. Table 7 and Figure 14 show the exhibition correctnesses got from cutting edge strategies, and the proposed model.

Notwithstanding the way that Toğaçar et al., (2020) study accomplishes a high exactness result when contrasted with different works, the proposed model accomplishes a cutthroat precision result and outflanks this work. In outline, the procedure used in this review is compelling for ordering and recognizing pneumonia sickness from Chest X-beam picture dataset, in light of the outcomes acquired from assessing the confirmation of idea.

Table 7: Comparison with state-of-the-art techniques

S/N	Authors	Model	Model Performance
1.	Ayan & Unver, 2019	VGG16	0.845
2.	Abiyev & Ma'aitah, 2018	CNN	0.9240
3.	Cohen et al., 2018	DenseNet-121	0.9280
4.	Stephen *et al.,* 2020	CNN	0.9531
5.	Chouhan et al., 2020	Ensemble of pretrained CNNs	0.9639
6.	Toğaçar *et al.,* 2020	Combined features of pretrained AlexNet, VGG-16, and VGG-19 with mRMR feature selection algorithm	0.9684
7.	The Proposed Model	CNN with Transfer Learning	0.986*

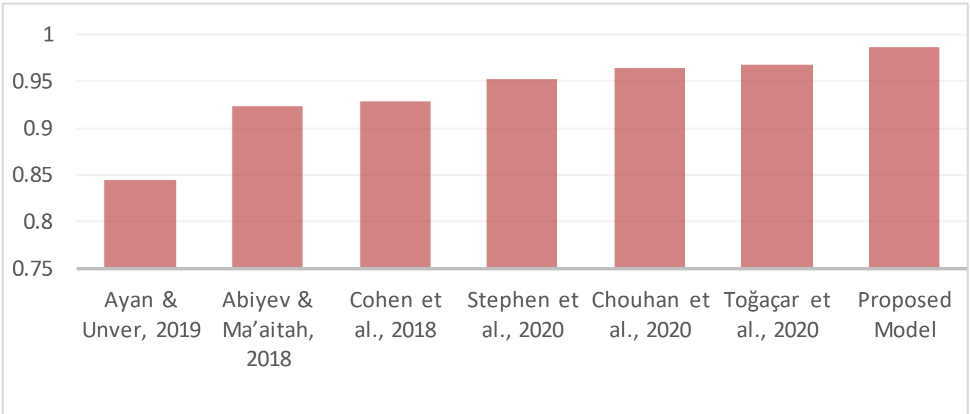

Figure 14: Comparison with state-of-the-art techniques

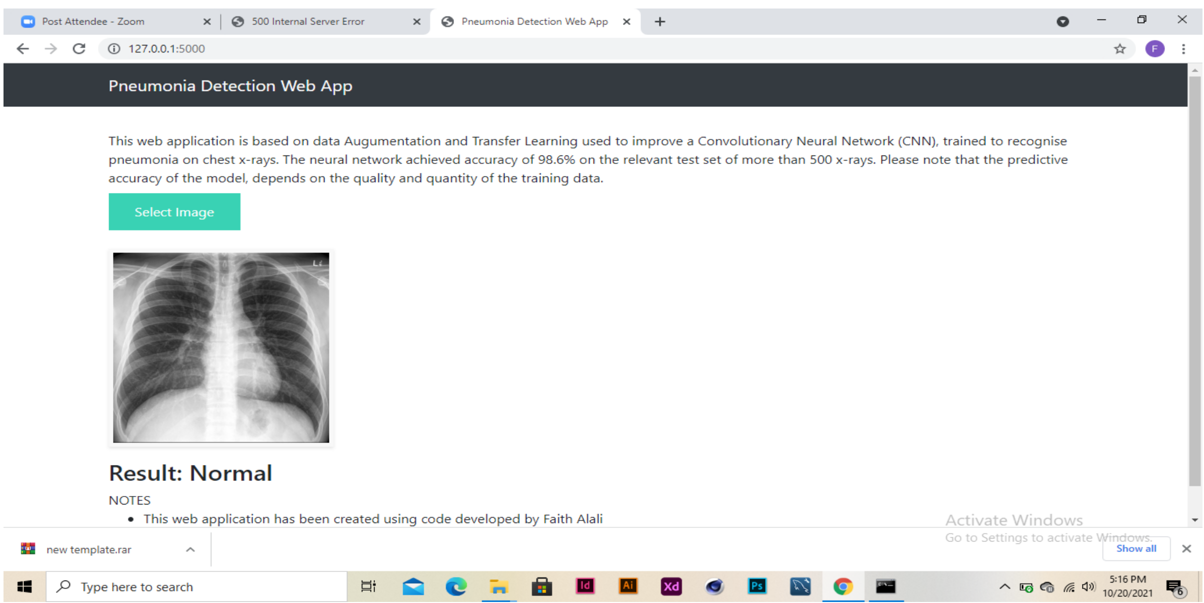

Figure 15: Result of Pneumonia detection using Chest X-ray image

International Journal of Recent Development in Engineering and Technology
Website: www.ijrdet.com (ISSN 2347-6435 (Online) Volume 15, Issue 08, August 2026)

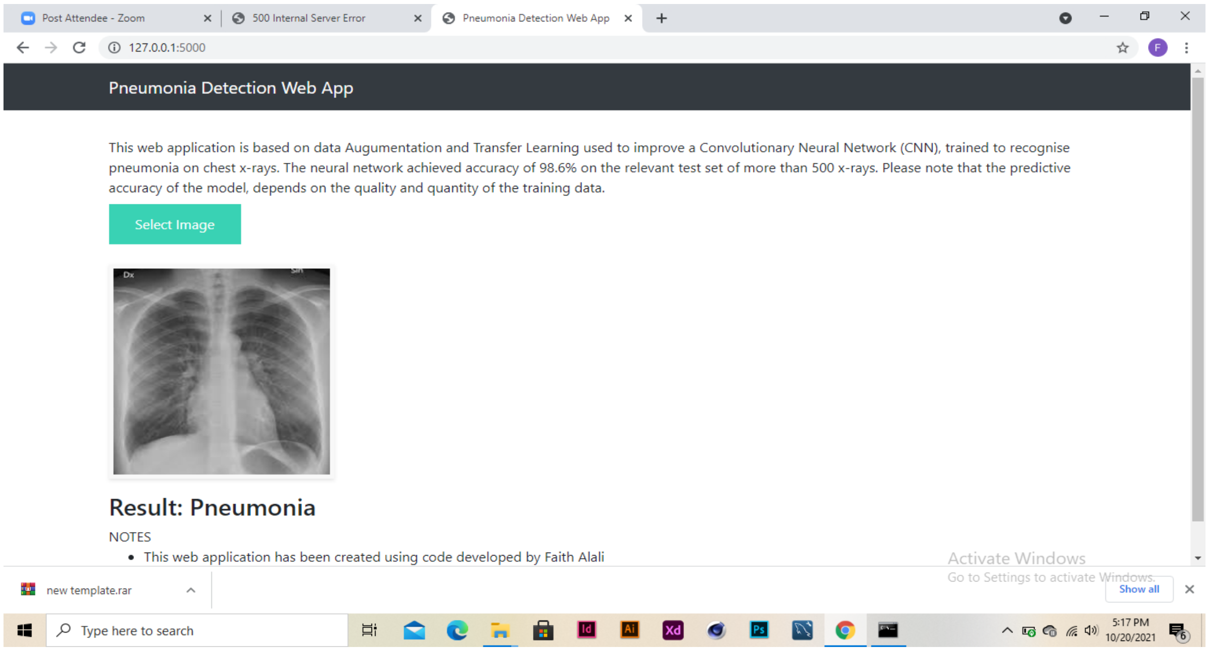

Figure 16: Result of Pneumonia detection using Chest X-ray image

V. Conclusion

This is the closing section of this research work, and it sums up and talks about the commitments of the review, and presents a viewpoint of the chances for future examination work. This review introduced a Deep learning structure for the assessment and discovery of pneumonia finding dependent on move learning and information increase. From the beginning the inspiration of this review was to address a portion of the difficulties that boundary around pneumonia finding particularly in African nations where there is lack of individuals who are talented in procedures like radiology. The aftereffects of the model exactness pace of 0.986 shows that our CNN model with move learning and information increase methods performs well in contrast with cutting edge profound learning design for pneumonia determination. To delineate the exhibition of our proposed model, the trial executed a few examinations of various information shapes and misfortune capacities were given. The exhibition of the executed model shows that the model could successfully order typical and unusual X-beams by and by. Thus, lessening the weight of radiologists. Likewise, the executed model can be increased to consequently separate between who need earnest clinical consideration and who can be made to pause too.

Hence, this review conveyed major information and increased calculations to work on the approval and arrangement exactness of the CNN model and also accomplished noteworthy execution precision which beat cutting edge CNN pneumonia analysis exiting models.

REFERENCES

[1] Akcay, S., Kundegorski, M., Devereux, M., & Breckon, T. (2016). Transfer learning using convolutional neural networks for object classification within X-ray baggage security imagery. 2016 IEEE International Conference on Image Processing (ICIP). doi: 10.1109/icip.2016.7532519

[2] Abiyev. (2018). Detection of pneumonia in chest X-ray images by using 2D discrete wavelet feature extraction with random forest. International Journal of Imaging Systems and Technology. doi: 10.1002/ima.22501

[3] Cohen N., Hussain, M., Al Adel, F., & Alzaidi, N. (2018). Deep learning based computer-aided diagnosis systems for diabetic retinopathy: A survey. Artificial Intelligence in Medicine, 99, 101701. doi: 10.1016/j.artmed.2019.07.009

[4] Ayan, E., & Unver, H. (2019). Diagnosis of Pneumonia from Chest X-Ray Images Using Deep Learning. 2019 Scientific Meeting on Electrical-Electronics & Biomedical Engineering and Computer Science (EBBT). doi: 10.1109/ebbt.2019.8741582

[5] Chouhan, V., Singh, S., Khamparia, A., Gupta, D., Tiwari, P., & Moreira, C. et al. (2020). A Novel Transfer Learning Based Approach for Pneumonia Detection in Chest X-ray Images. Applied Sciences, 10(2), 559. doi: 10.3390/app10020559

[6] Christodoulidis, S., Anthimopoulos, M., Ebner, L., Christe, A., & Mougiakakou, S. (2017). Multisource Transfer Learning With Convolutional Neural Networks for Lung Pattern Analysis. IEEE journal of biomedical and health informatics, 21(1), 76–84. https://doi.org/10.1109/JBHI.2016.2636929

[7] Deng, J., Dong, W., Socher, R., Li, L., Kai Li, & Li Fei-Fei. (2009). ImageNet: A large-scale hierarchical image database. 2009 IEEE Conference on Computer Vision and Pattern Recognition. doi: 10.1109/cvpr.2009.520684

[8] El-Sayed, A., El-Dahshan, H.M., Mohsen, K. R., & Abdel-Badeeh, M.S. (2020). Computer-aided diagnosis of human brain tumor through MRI: A survey and a new algorithm. Expert Systems with Applications, 41(11), 5526-5545.

[9] Elshennawy, N., & Ibrahim, D. (2020). Deep-Pneumonia Framework Using Deep Learning Models Based on Chest X-Ray Images. Diagnostics, 10(9), 649. doi: 10.3390/diagnostics10090649

[10] Kelly, J. (2022). How Artificial Intelligence is Changing Radiology, Pathology. Retrieved 7 March 2021, from https://healthitanalytics.com/news/how-artificial-intelligence-is-changing-radiology-pathology.

[11] Kieu, P., Tran, H., Le, T., Le, T., & Nguyen, T. (2018). Applying Multi-CNNs model for detecting abnormal problem on chest x-ray images. 2018 10Th International Conference On Knowledge and Systems Engineering (KSE). doi: 10.1109/kse.2018.8573404

[12] Knok, Ž., Pap, K., & Hrnčić, M. (2021). Implementation of intelligent model for pneumonia detection. Tehnički Glasnik, 13(4), 315-322. doi: 10.31803/tg-20191023102807

[13] Labhane, G., Pansare, R., Maheshwari, S., Tiwari, R., & Shukla, A. (2020). Detection of Pediatric Pneumonia from Chest X-Ray Images using CNN and Transfer Learning. International Conference on Emerging Technologies in Computer Engineering: Machine Learning and Internet of Things (ICETCE). doi: 10.1109/icetce48199.2020.9091755

[14] Militante, V.S, & Sibbaluca, G.B. (2020). Pneumonia Detection using Convolutional Neural Networks. International Journal of Scientific & Technology Research, 9(04)

[15] Panch, T., Szolovits, P., & Atun, R. (2020). Artificial intelligence, machine learning and health systems. Journal of Global Health, 8(2). doi: 10.7189/jogh.08.020303

[16] Pan, S., & Yang, Q. (2019). A Survey on Transfer Learning. IEEE Transactions on Knowledge and Data Engineering, 22(10), 1345-1359. doi: 10.1109/tkde.2009.191

[17] Stephen, O., Sain, M., Maduh, U., & Jeong, D. (2020). An Efficient Deep Learning Approach to Pneumonia Classification in Healthcare. Journal of Healthcare Engineering, 2019, 1-7. doi: 10.1155/2019/4180949.

[18] Togar W. (2020). Can machine-learning improve cardiovascular risk prediction using routine clinical data? PLOS ONE, 12(4), e0174944. doi: 10.1371/journal.pone.0174944